

# JOINT INSTITUTE FOR AERONAUTICS AND ACOUSTICS



Stanford University

JIAA TR - 101

National Aeronautics and  
Space Administration

Ames Research Center

## Forebody Tangential Blowing for Control at High Angles of Attack -Feasibility Study Final Report

AMES GRANT  
1N-08-CR  
37754  
p. 42

By

I. Kroo and L. Roberts

Stanford University  
Department of Aeronautics and Astronautics  
Stanford, CA 94305

June 1991

(NASA-CR-188773) FOREBODY TANGENTIAL  
BLOWING FOR CONTROL AT HIGH ANGLES OF ATTACK  
Final Report (Stanford Univ.) 42 PCSC 01C

46

N91-30152  
541495  
Unclas  
63/08 0037754

# **Forebody Tangential Blowing for Control at High Angles of Attack**

## **—Feasibility Study Final Report**

I. Kroo, S. Rock, and L. Roberts  
Stanford University

### **Introduction**

This report summarizes work performed under NASA grant NCC2-55. The project was started in the summer of 1989. It consisted of a feasibility study, intended to ascertain whether the use of tangential leading edge blowing over the forebody could produce effective and practical control of the F-18 HARV aircraft at high angles of attack.

The work consisted of the following phases:

1. Aerodynamic Modeling — A simplified model of the F-18 configuration using a vortex-lattice model was developed to obtain a better understanding of basic aerodynamic coupling effects and the influence of forebody circulation on lifting surface behavior. The effect of tangential blowing was estimated using existing wind tunnel data on normal forebody blowing and analytical studies of tangential blowing over conical forebodies. From this review of previous work, vehicle forces and moments due to blowing over a range of angles of attack and blowing rates were estimated.
2. Control system design — Incorporation of forebody blowing into the flight control system was investigated by adding this additional yaw control and sideforce generating actuator into the existing F-18 HARV simulation model. A control law was synthesized using LQG design methods that would schedule blowing rates as a function of vehicle sideslip, angle of attack, and roll and yaw rates. This control system was "wrapped around" the existing closed-loop F-18 model and the resulting enhanced vehicle was simulated using the nonlinear NASA HARV simulation program. Vehicle response to blowing commands and closed-loop time histories of the vehicle at high angles

of attack with sideslip perturbations were predicted. Cases with and without blowing control revealed that the range of controllable angle of attack could be extended significantly with the addition of blowing control. Required blowing rates were found to be smaller than other types of blowing control.

3. Implementation — Based on the estimated blowing momentum coefficients required for flight control at high angles of attack, possible schemes for obtaining this flow rate were explored. Three alternatives were considered: compressed or liquefied gas bottle, APU or auxiliary compressor, and engine bleed air. Required values of  $C_{\mu}$  were translated into mass flows based on assumed geometric constraints and choked slot flow. Despite the relatively low momentum coefficients, a reasonable test period could not be obtained with the use of the first two alternatives, but data obtained from G.E. indicated that sufficient engine air is available to provide the desired blowing rates.

4. Feasibility demonstrator — Because of the highly nonlinear flow field and important coupling with the vehicle dynamics, an inexpensive flight research vehicle to test the basic concept was developed. The vehicle was tested in a wind tunnel at Stanford University, with results to be reported subsequently.

The conclusion of this short study is that the proposed concept is feasible. The work has identified areas in which additional experimental data is needed and has suggested fruitful topics for future analysis.

### **Objectives and Approach**

The objective of this short study was to demonstrate how forebody blowing might be used to increase aircraft maneuverability. In particular, the investigation focussed on the feasibility of a forebody blowing system on the NASA F-18 HARV Aircraft.

The approach involved parallel efforts in the areas of aerodynamics and controls. An aerodynamic

model of the vehicle was developed based on existing experimental data and a simple flow solver. Work was undertaken to identify the range of flow conditions over which this approach would be useful.

A demonstration control system was designed based on the NASA Dryden HARV simulation and an LQR control law. The closed loop simulation was run at high angles of attack to demonstrate the loss of lateral control without blowing and the reestablishment of controlled flight with fore-body blowing control.

Since much of the available data was classified during this work, it was decided that additional data could be obtained using a scale model. Flight or wind tunnel testing on this model could provide important data required for control law design. The airframe was designed, a blowing system designed, constructed and tested, and a sensor / control system was developed. Although the vehicle was not flown freely, it was tested in a wind tunnel at Stanford.

Finally, a feasibility study was undertaken to determine whether the system could be installed on the F-18 aircraft. This involved estimates of required mass flow and determination of how this could best be generated.

## **Aerodynamic Modeling**

### *Theoretical Investigation*

To understand the origin of some of the basic aerodynamic forces and moments relevant to the control law design, a vortex lattice model was developed and is shown in figure 1. Results are shown in figure 2. As might be expected, the lift is rather well predicted out to angles of attack of  $30^\circ$  or more. The general trend of sideforce at  $20^\circ$  of sideslip is properly predicted although the magnitude is underestimated. Pitching moment is also reasonably predicted even at these large sideslip angles; however, rolling moment and especially yawing moment depart from the measured values at angles of attack above about  $20^\circ$  for this model. The use of reduced circulation models for post-stall were investigated with the conclusion that fuselage vortex shedding was particularly important to accurate computation of yawing moment. A better model with free vortex wakes on the fuselage would be needed to significantly improve the prediction.

Several coupling effects can be modeled by introducing streamwise circulation at forebody as a representation of the effects of blowing. In addition to a direct sideforce and its associated yawing moment, the trailing vorticity produces a nonlinear roll coupling by increasing the asymmetric downwash distribution on the wing and introducing a sidewash on the vertical tail surfaces. (See figure 3.)

### *Experimental Investigation*

Clearly, a detailed experimental database would be useful for the control system modeling. However, the primary data obtained at NASA Ames Research Center on the P-600 model was classified just after the current program started. Other available data was limited, but indicated that the primary effect of forebody blowing is associated directly with the forebody sideforce. (Figure 4.) Data that has now been made available indicates large available yawing moments, increasing with angle of attack (Figure 5.)

As suggested by the vortex lattice calculations, significant  $C_{n\alpha}$ ,  $C_{y\alpha}$ ,  $C_{l\alpha}$  terms appear with asymmetric blowing. This produces a strong coupling of longitudinal and lateral dynamics, requiring more careful control system design. The  $\alpha$  - dependence is due primarily to the fact that the sideforce is produced by cross-flow on the fuselage so that with blowing we expect a  $\sin \alpha$  variation in sideforce and yawing moment.

### *Summary*

The fundamental effect of forebody blowing is on yawing moment. The effectiveness increases with angle of attack, unlike the rudder effectiveness which becomes quite small at higher angles of attack. However, other forces and moments are also produced including: sideforce in the opposite direction as a rudder would produce for a given yawing moment, highly nonlinear rolling moments associated with downwash on the wings and interference with the vertical tail surfaces, and nonlinear rate derivatives. From the vortex lattice model, it is expected that further coupling between longitudinal and lateral motion will result from yawing moment due to pitch rate and pitching moment due to yaw rate.

## Control System Design

### *Philosophy*

One of the major issues determining the feasibility of using any pneumatic control system is its mass flow requirement. Consequently, an attempt has been made to approximate the requirements of the proposed system for the F/A 18.

The procedure employed to develop the approximation was to design a yaw control system that could be installed as outer loop around the existing F/A 18 flight control system. This control logic was then implemented and tested in the full nonlinear HARV simulation. Details of the implementation are provided in the following section.

A schematic of the proposed proof-of-concept control system is presented in Figure 6. One justification for this approach is that such a system should require even less mass flow. The non-optimality results from the lack of coordination in the design between the blowing system and the other yaw effectors.

There are other advantages to this approach. One of the greatest is that it is easy to design and implement. Since the system is intended only to augment the stability of an existing system, there is no need to address the complexities of a complete flight control system. Ease of implementation is also included as part of this benefit.

Another advantage is that treating the pneumatic control as an outer loop allows similar designs to be implemented on different aircraft systems. For example, similar yaw augmentation systems could be implemented on a real aircraft and on a remote controlled model aircraft. The latter would could be done to provide a low cost proof-of-concept flight test demonstration.

Note that there is no claim that an outer loop configuration would represent the final configuration. In fact, the final configuration envisioned would result from complete redesign of the entire flight control system. Only in this way can the actions of the pneumatic control and the aerodynamic surfaces be coordinated efficiently. Another reason for addressing a complete flight control design is that pneumatic systems to control vortex behavior are inherently nonlinear. They cannot

properly be treated as yielding incremental forces and moments as is often done with the aerodynamic surfaces. When activated, pneumatic control and the effectiveness of the other effectors (e.g. if the vortex flow is altered, the effectiveness of an aileron can be altered drastically). At the extreme, the entire concept of using stability derivatives to describe an aircraft becomes questionable.

For these reasons, developing optimal or efficient use pneumatic control systems may require extensions to the state-of-the-art in nonlinear flight control system design. There is exciting research potential. The justification for such research, however, depends on there being sufficient performance improvements for the aircraft system. Demonstrating the potential for such improvements is the goal of addressing the simple control logic described in Figure 6.

### *Control Law Design*

Using blowing to control the vortex flow and hence produce a yawing moment is conceptually an appealing concept. At high angles-of-attack such an effector is potentially very powerful whereas the effectiveness of conventional aerodynamic surfaces is greatly diminished. In fact, the existing F/A-18 exhibits an instability (large amplitude limit cycle) at approximately  $45^\circ$  angle of attack. The source of this instability is apparent in Figure 7. Plotted are the  $C_n$  stability derivative (yawing moment) and the rudder effectiveness,  $\partial C_n / \partial \delta_r$ , versus angle-of-attack and that the rudder effectiveness drops rapidly at  $20^\circ$  and even more at  $45^\circ$ . The significance of this is that the control system relies on the rudder to compensate for the radical change in  $C_n$ , and the rudder loses its effectiveness at high angle-of-attack. Augmenting the control system with an effector (blowing) that increases in effectiveness at high angles-of-attack offers the promise of greatly increasing the flight-maneuver envelope of the aircraft.

One potential complicating factor in using forebody blowing (as viewed by the controls engineer) is that it acts in front of the center-of-gravity rather than behind it (as does the rudder). This results in a non-minimum phase system characterized by a zero in the right-half of the s-plane. Such systems are typically more difficult to control. In this effort, the result was that all attempts to design simple controllers using only beta (and its derivatives) as feedback were unsuccessful (note that the

effort was limited, however). Rather, a full state linear quadratic design was accomplished that fed back  $\beta$ ,  $r$ ,  $p$ , and  $\phi$ .

A typical pole-zero pattern for a transfer function from blowing input to yaw-angle output is shown in Figure 8. The right-half plane zeros are apparent. This figure was obtained by extracting a linear model of the closed-loop F/A-18 from the HARV simulation (see next section). For this derivative, blowing was modeled as a stability derivative increment. The values used are presented in Table 1. Values for the rudder are included for comparison. Note the sign change on the  $C_Y$  derivative. The state variable mode of the closed loop system using  $\beta$ ,  $r$ ,  $p$ , and  $\phi$  as states is:

$$\begin{bmatrix} \dot{\beta} \\ \dot{r} \\ \dot{p} \\ \dot{\phi} \end{bmatrix} = \begin{bmatrix} -.0971 & .2290 & .1037 & -.9722 \\ -10.2147 & -1.0287 & -.1111 & .6408 \\ 0 & 1.0 & 0 & .2350 \\ .8613 & -.0070 & .0202 & -.1044 \end{bmatrix} \begin{bmatrix} \beta \\ r \\ p \\ \phi \end{bmatrix} + \begin{bmatrix} -.0017 \\ .0148 \\ 0 \\ -.0591 \end{bmatrix} C_{\mu}$$

This fidelity of this linear model is marginal. Its response to a step in blowing is compared with the full HARV simulation's response in Figure 9. Clearly, improvements in the model are necessary, but this was beyond the scope of the current effort. All that was required for this study was a model that predicted general trends so that a candidate control logic could be designed.

The design of the actual control system that was implemented was accomplished using this model and PC-MATLAB. The result is:

$$C_{\mu} = 469*\beta - 65*p - 81*\phi - 196*r.$$

Again, no claim is made that this is a *good* control design. Rather, this is *a* control design that when applied to the HARV simulation, stabilized the motion at high alpha. The derivation of the control gains is relatively unimportant. Future work will address the fidelity of the model and the development of better control logics.

Results showing the performance of this control logic when applied to the HARV simulation are presented in following sections.



### *Simulation*

The simulation used for this study was a modified version of the real-time HARV simulation used at NASA Ames Dryden Flight Research Center. The simulation and a set of validation results were provided by NASA. The simulation was modified at Stanford to incorporate the effects of forebody blowing and to run on an IBM compatible personal computer under DOS.

The major modifications included:

- (1) The main program which controls program flow was rewritten to operate on a single computer in a batch mode rather than on multiple processors in real time (as is done at NASA).
- (2) The input routines were rewritten to accept time histories of stick and pedal inputs rather than process real time signals.
- (3) The output routines were rewritten to create ASCII data files that could be processed off-line to create plotted output. PC-MATLAB was the program used to process the data and create the plots.
- (4) The initialization loop was rewritten.
- (5) The capability (preliminary) to extract linear models of the closed-loop aircraft was added.
- (6) The effects of forebody blowing and a control system to govern its use were added.

Given the above modifications, the program has a 502K executable image. Current limitations of the PC version of the simulation include:

- (1) Only the "clean" and the "high-alpha" data bases have been implemented. The "takeoff" and "approach" data bases were eliminated to reduce memory requirements.
- (2) No hinge moment data are incorporated. This was a result of not having a valid data base soon enough in the effort. The data are now available and could be added easily.

## *Results*

Two test cases were run to demonstrate the effectiveness of the control logic defined in the previous section. Again, the goal was to obtain a rough estimate of the amount of blowing that was required rather than to evaluate the control system.

The first case was designed to demonstrate nominal (good) performance of the F/A-18 in a "normal" part of its flight-maneuver envelope. A pedal doublet applied to an aircraft trimmed at  $13^\circ$  angle-of-attack (altitude = 10K ft, velocity = 300 ft/sec) was chosen. The results are presented in Figure 10. The aircraft is well behaved.

The second case chosen was a pedal doublet applied at  $45^\circ$  angle-of-attack. The results of the nominal closed-loop F/A-18 are presented in Figure 11. Note that the aircraft response is unstable. also note that the aircraft was "flown to"  $45^\circ$  using the longitudinal stick since it was not possible to trim the aircraft at that attitude with centered control stick.

Figure 12 presents data for the same condition as Figure 11 except that the blowing control law was activated at roughly seven seconds into the transient (in order to allow the beta response to build). Note the excellent response in returning the system to zero when the blowing is activated. Note also that the amount of mass flow required by the blowing system to perform this maneuver was well within the reasonable limits described in the section on full scale implementation.

The conclusions to be drawn from figure 12 include:

- (1) Blowing on the forebody of an F/A-18 is a very effective means of producing yawing moment control at high angles of attack, and
- (2) The predicted mass flow requirements of such a system are well within reasonable limits.

Future work is required to develop and incorporate more accurate descriptions of the effects of blowing into HARV simulation, and to address the complex issues of designing control systems that will incorporate blowing.

## **F-18 Model Development**

### *Objectives*

A scale model of the F-18 was constructed to demonstrate the effectiveness of forebody blowing for yaw control at high angles of attack. It was planned that this model would be flown, or at least tested, to provide additional aerodynamic data for control law design, to permit preliminary evaluation of control strategy, and to obtain unsteady aerodynamic data.

### *Description*

The model airframe was based on a Byron Originals R/C model kit and consisted of a molded fiberglass fuselage and Styrofoam wing and tail surfaces with aluminum spars. The model was powered by an O.S. 0.91 ducted fan. The control system consisted of a PWM R/C system, a Futaba rate gyro, and a "Tattle-Tale" computer. Interfaces for these systems were developed and tested during the course of this research program.

The blowing system consisted of an electrically-powered centrifugal compressor, constructed specially for this model. Blowing slots were constructed in the forebody and the plenum was constructed of fiberglass and polyester resin. This design was developed after initial tests of a Freon propellant system yielded unsatisfactory results. A revised system using "Propel" as a working fluid was then constructed and evaluated. This too was insufficient to generate the required 60-100

seconds of blowing with  $C_{\mu} = .003$ . Methods for using "bleed" air from the ducted fan were considered, but the final solution used a separate centrifugal compressor driven by an Astro-5 electric motor and Ni-Cad batteries. (Figure 13.)

### *Tests*

Tests of the subsystems, including electronics, blowing system, and wing-leveling autopilot were completed successfully, but due to time constraints, the planned flight tests were replaced with a wind tunnel investigation. Results of these tests (see installation photo in figure 14) will be reported subsequently.

## **Full-scale Implementation — Feasibility Study**

### *Introduction*

The successful mechanical implementation of an active yaw control blowing system for the F-18 is vital to this study. Also, as in all aeronautical design studies, weight and size considerations are always in the forefront. Three methods for implementation of this section of the report. The basis of this study is the basic requirements and limitations imposed to obtain a viable solution of the design problem. These basic requirements are listed first, followed by a description of each of the three methods. The methods are: (1) using bottled liquid gas, (2) using the auxiliary power unit (APU) and, (3) using bleed air from the engine. Finally a conclusion is given with recommendations for further work.

### *Basic requirements and limitations*

Proposed flight conditions:

Altitude:	10,000 ft
CL:	1 to 1.8
Load factor (L/W):	1

Aircraft statistics:

Fighter configuration weight: 15740 kg (34700 lb)

Blowing jet data:

Jet Mach number:	0.7
Slot length:	6 -8 ft
Max slot height:	5 -10 mm
Time of blowing:	5 -10 min.

Other considerations applicable to a bottled system or one with an intermediate plenum, are weight and space. Weight considerations include stability data like longitudinal and lateral distances from center of gravity, aerodynamic center and center of pressure. Space considerations include the existing availability and possible availability of space for storage of these devices. Coupled to this is the necessity of plumbing to bring the control gas to the jet slot.

Considerations not addressed in detail in this report include:

- the controllability of the jet (response time, repeatability of velocity, momentum at different altitudes)
- steadiness of supply/reservoir conditions (temperature, pressure, mass flow) during operation of jet.

#### *Defining equations and definitions*

The blowing momentum coefficient is defined as follows

$$C_{\mu} = m V_j / (qS) \quad (1)$$

The mass flow,

$$m = \rho_j V_j A_j \quad (2)$$

Thus, the area of the jet slot:

$$A_j = C_{\mu} q S / (\rho_j V_j^2) \quad (3)$$

From the definition of the lift coefficient:

$$L = qS C_L \quad (4)$$

With  $L/W = 1$ :

$$q S = W / C_L \quad (5)$$

where  $W$  is the weight of the aircraft.

Sound speed of the gas,

$$c_j = \sqrt{\gamma R T_j} \quad (6)$$

Pressure ratio across an isentropic nozzle as a function of nozzle Mach number,

$$P_0 / P = [1 + M^2 (\gamma - 1) / 2] ^{\gamma / (\gamma - 1)} \quad (7)$$

### *Proposed Systems*

#### CO<sub>2</sub> Bottled Gas System

The primary parameters to be determined in this case are the required mass flow and thus the weight and size of the required storage bottle. To do this we need the thermodynamic and thermophysical properties of CO<sub>2</sub>.

Fig. 15 shows a pressure-enthalpy diagram for CO<sub>2</sub>, also known as Refrigerant 744. Note that liquid CO<sub>2</sub> implies that we have a thermodynamic equilibrium state somewhere on the liquid saturation line, the exact pressure and density depending on the temperature of the storage bottle.

Since the jet exit is at atmospheric pressure (which depends on the altitude), this is the final reference condition assuming that the jet pressure is the same as atmospheric. Since it is required to have a subsonic velocity at the jet, the pressure ratio across the jet needs to be controlled for this to be so.

By specifying the jet exit Mach number, we have already assumed a certain pressure ratio across an 'isentropic' nozzle for a given jet exit temperature.

A program was written (see Appendix) in which the user specifies the following input parameters:

- \* Blowing momentum coefficient
- \* CL for typical control maneuver
- \*  $L/W$
- \* Weight of aircraft
- \* Altitude
- \* Jet Mach number
- \* Jet exit temperature
- \* Jet slot length
- \* Required blowing time
- \* Reservoir storage temperature

The following parameters are then calculated using the defining equations and table look-ups:

- \* Jet exit velocity
- \* Exit density
- \* Exit area, slot height
- \* Jet mass flow rate
- \* Initial mass required
- \* Initial volume required
- \* Pressure ration required across isentropic nozzle

For the above assumption of constant reservoir conditions we need to determine what the required heat input rate is for this assumption to be valid. In the reservoir, liquid  $\text{CO}_2$  is continually being vaporized to gas. This requires heat of vaporization which needs to be supplied externally if not available from the surroundings. With reference to Fig. 15, the enthalpy-pressure diagram for  $\text{CO}_2$ , this amount of specific heat can be identified as the horizontal distance between the two legs of the saturation curve. From the tabulated values of enthalpy of different temperatures, and the calculated mass flow, we can calculate the heat input required. This was also included in the program.

Table 2 shows the calculated parameters for a range specified by the basic requirements.

As can be seen from the table, this is not a viable solution to the problem. The obvious reason is that the mass flow rate required results in too heavy and large a reservoir. A secondary reason is the large amount of heat required for a constant temperature reservoir also due to the large mass flow rate.

#### Using Auxiliary Power Unit (APU)

The next option is to use the APU. This 200 kW unit is a Garrett Ai Research turbine used for starting one engine of the F-18 and for testing of the systems before take-off. It is also used to some extent for environmental control during flight. The following data on the exit air of the APU is available:

Exit pressure: 33.3 - 55.5 psig (3.31 - 4.90 bar abs)

Entrance temperature: 1236° ± 15° F (942° ± 8° K)

This supply air has too much energy for direct expansion across a nozzle and would therefore need some intermediate plenum. The most important factor in evaluating this option, however, is the available mass flow rate. This number was not available and was crudely, optimistically estimated as follows:

If this air should exhaust isentropically with no losses, the following isentropic relation determines the final temperature:

$$T_{02} - T_{03} = T_{02} [ 1 - P_a / P_{02} ]^{(\gamma-1) / \gamma} \quad (8)$$

The specific work available is then

$$W = c_p (T_{02} - T_{03}) \quad (9)$$

Again with no losses, the mass flow rate, given the power output

$$\dot{m} = P/W \quad (10)$$

Choosing representative conditions as 942°K, 3.3 and 4.9 bar, and  $c_p = 1005 \text{ kJ/kgK}$  we get mass flow rates of 0.73 and 0.58 kg/s respectively. The program described in the previous section was run with air as control gas, with the results presented in table 3.



It can be seen that the mass flow rates required for the specified blowing momentum coefficient are considerably more than that available from the APU. This makes this option only viable if an intermediate reservoir is used which is pumped up with excess air when the control system is not in use. This is a topic for future research.

#### Bleed air from the engines

The final alternative discussed in this section is that of using air from the aircraft's engines. Possibilities include normal bleed air and "anti-ice" bleed air. Normal bleed air is bled off the engine in the last stages (7) of the high pressure compressor. Anti-ice air comes from stage 4 of the high pressure compressor. Both supplies are relatively high temperature but since they are bled off before the burner, are clean without products of combustion.

For a typical maneuver specified under the basic requirements,

Altitude: 10 000 ft

Angle of attack: 45°

Flight Mach number: 0.6

The throttle position, available bleed air and thermodynamic conditions are displayed in table 4. (PLA = Power Level Angle).

Normal bleed air is 6% of W1. 'Anti-ice' bleed air is 0.8% of W25.

Table 5 shows the available normal bleed air and table 6, the available air from the anti-ice system. Comparing with the required values presented in table 3, we are now in the right order of magnitude using the normal bleed air, but not the 'anti-ice' bleed air.

This air needs to be brought down in temperature and pressure before it reaches the jet slots if a subsonic jet is required.

## *Summary*

1. It was shown in this section of the report that implementation of a blowing system to control the yawing moment is viable if the normal bleed air from the engines can be used.
2. Other systems using bottled gas or the APU are shown to be inadequate due to a too low mass flow rate.
3. Next steps in the design of the mechanical system implementing this idea would include:
  - design of the jet nozzle shape and plenum cross-section for 'isentropic' flow
  - layout of plumbing and valves required to bring the air to the nose of the aircraft.
  - determination of the lag-effects due to the length of ducting
  - linkage of the actuation of the valves to the control system of the aircraft

## **Conclusions**

In summary, the following conclusions may be drawn from this brief investigation:

- Tangential forebody blowing can significantly extend the controllable angle of attack range of the F-18 aircraft.
- Several aerodynamic nonlinearities and couplings have been identified and should be the subject of continued investigation.
- Blowing system requirements for both model and full-scale aircraft were evaluated: mass flow rates are critical factors, but can be achieved.

## **Future Work**

Many topics have been identified as beyond the scope of this initial investigation, but may be crucial for continued development of the concept. These include:

- Improved aerodynamic prediction methodology
  - Post-stall prediction capability
  - Unsteady effects
- Acquisition of additional aerodynamic data
  - Classification problem
  - Future tests
- Refined control law development
  - Gain scheduling
  - Coupling effects ( $C_{\mu}$  modifies derivatives)
- Continued RPV construction and testing
- Full-scale blowing system integration issues
  - Ducting system requirements
  - Reduced mass flow slot design

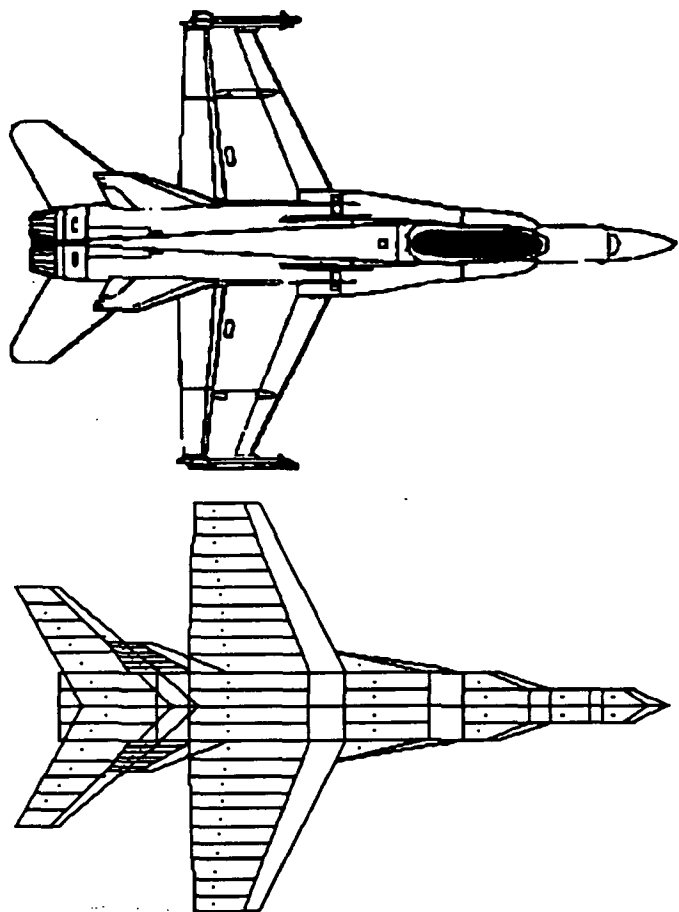


Figure 1. Vortex lattice representation of F-18.

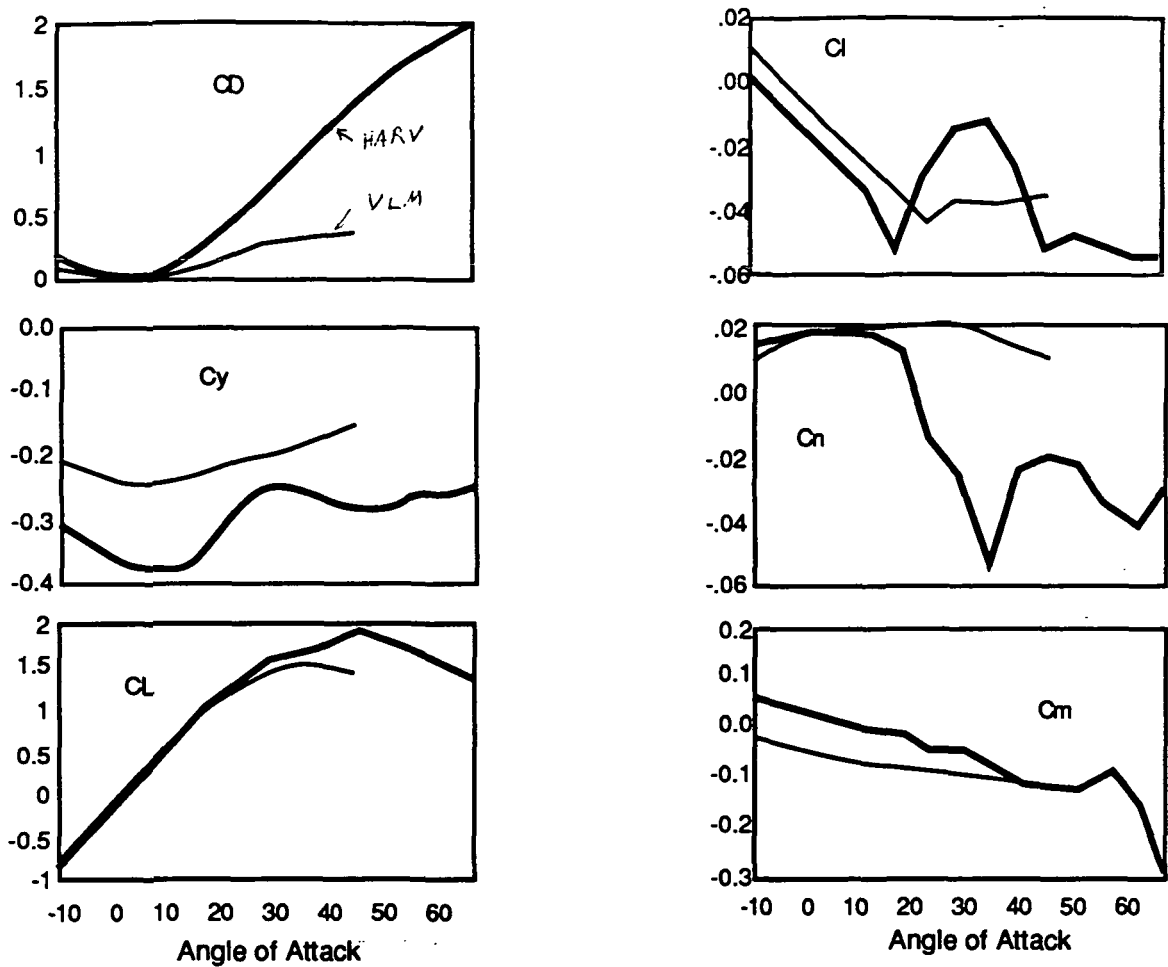


Figure 2. Comparison of computed aerodynamic characteristics using a simple vortex lattice model with NASA HARV Aero Model Database. Beta = 20°, C.G. at 33.6 ft from nose.

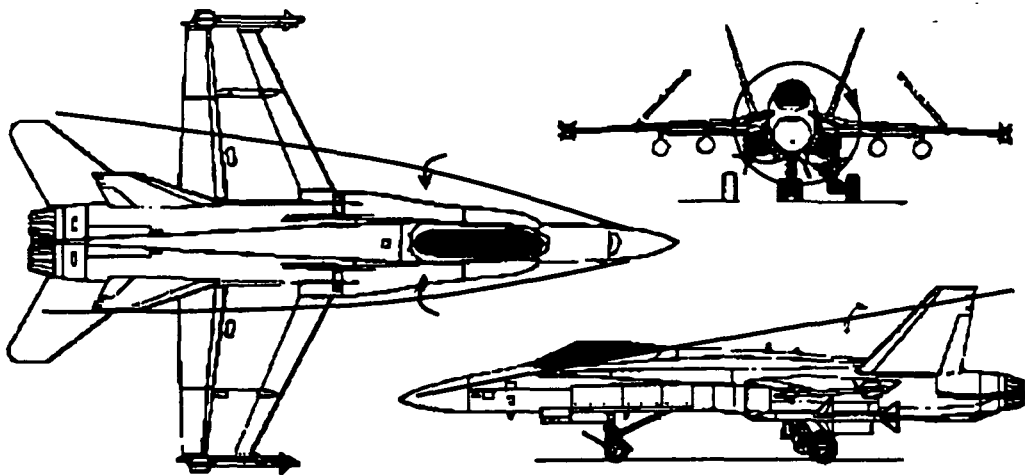
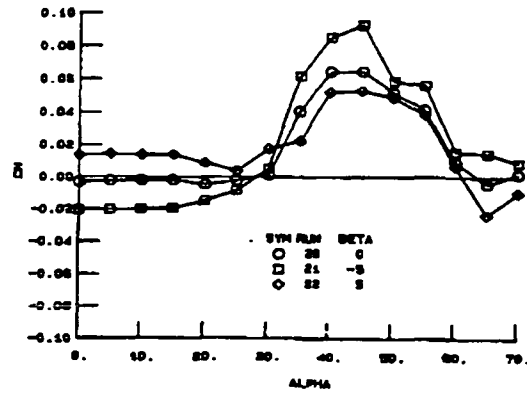
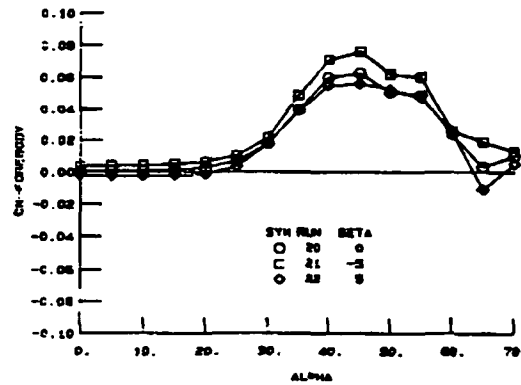


Figure 3. Blowing Effects on Forces and Moments.



a. Complete configuration



b. Forebody contribution to complete configuration

Figure 4. Experimental data using other blowing schemes suggests that most of the yawing moment is produced by local sideforce on the fuselage.

## Estimated Effects of Blowing

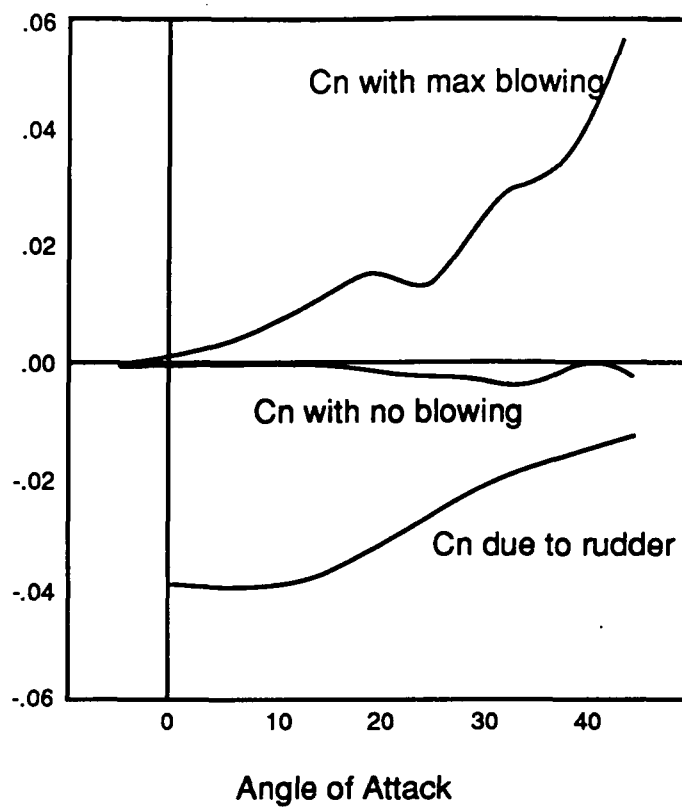


Figure 5. Effect of blowing on yawing moment.



Derivative	Rudder (per deg)	Blowing (per .001 $C_\mu$ )
$\partial C_l / \partial \delta_r$	0.00028	0.0
$\partial C_m / \partial \delta_r$	0.00011	0.0
$\partial C_n / \partial \delta_r$	-0.0012	-0.007
$\partial C_D / \partial \delta_r$	0.000	0.0
$\partial C_L / \partial \delta_r$	0.000	0.0
$\partial C_Y / \partial \delta_r$	0.0038	-0.016

Table 1. Assumed stability derivative increments due to rudder and blowing.

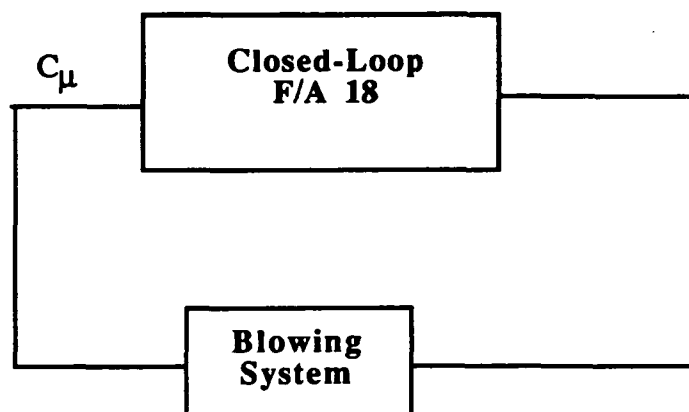


Figure 6. Implementation of blowing scheme as outer loop around existing F-18 system.

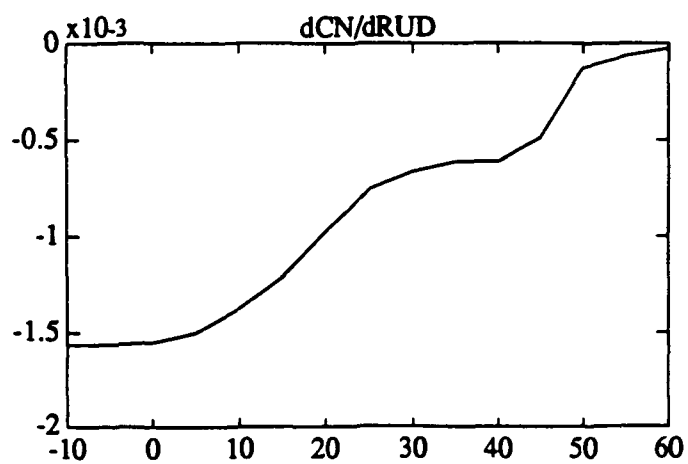
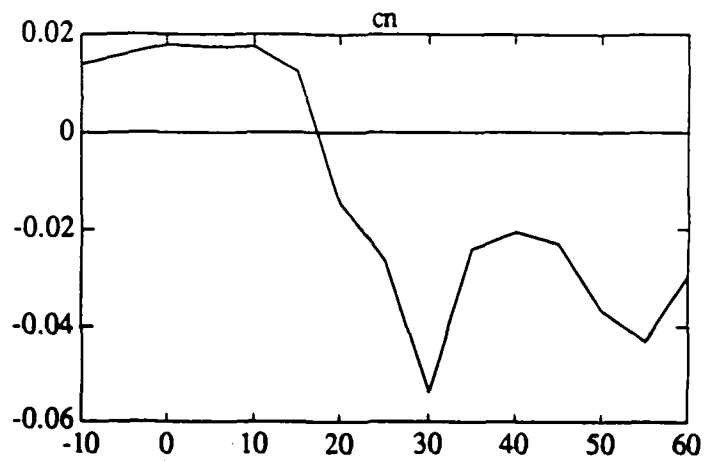


Figure 7. Yaw stability and control characteristics for F-18 vs. angle of attack.

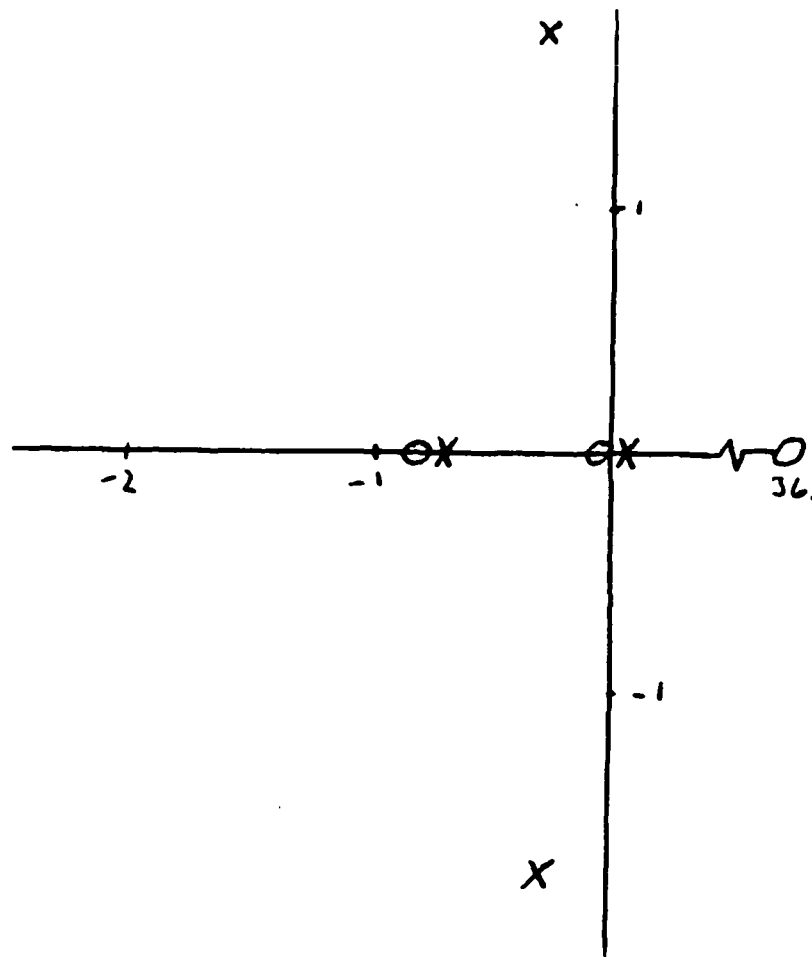


Figure 8. Typical pole-zero pattern for blowing input to yaw angle output.

## HARV SIMULATION VS LINEAR MODEL

---

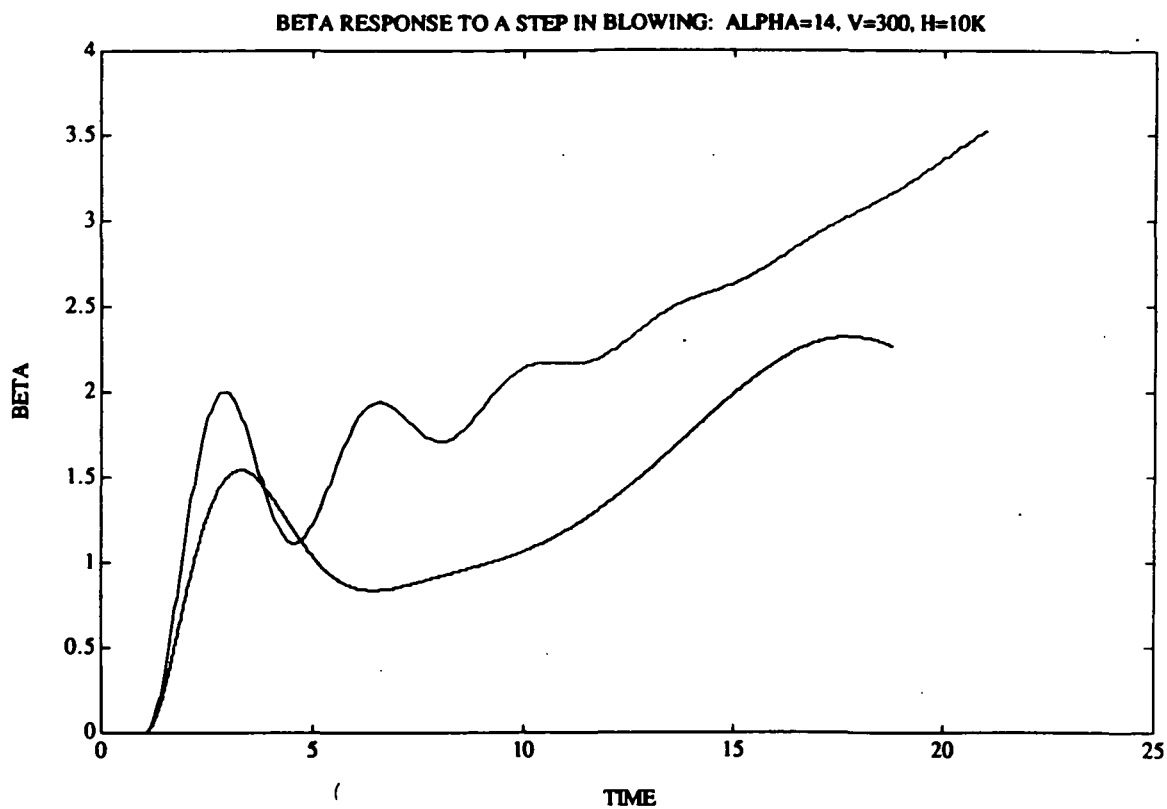


Figure 9. Comparison of linear model and HARV simulation — response to step input in blowing.

## PERFORMANCE OF HARV AT 13 deg

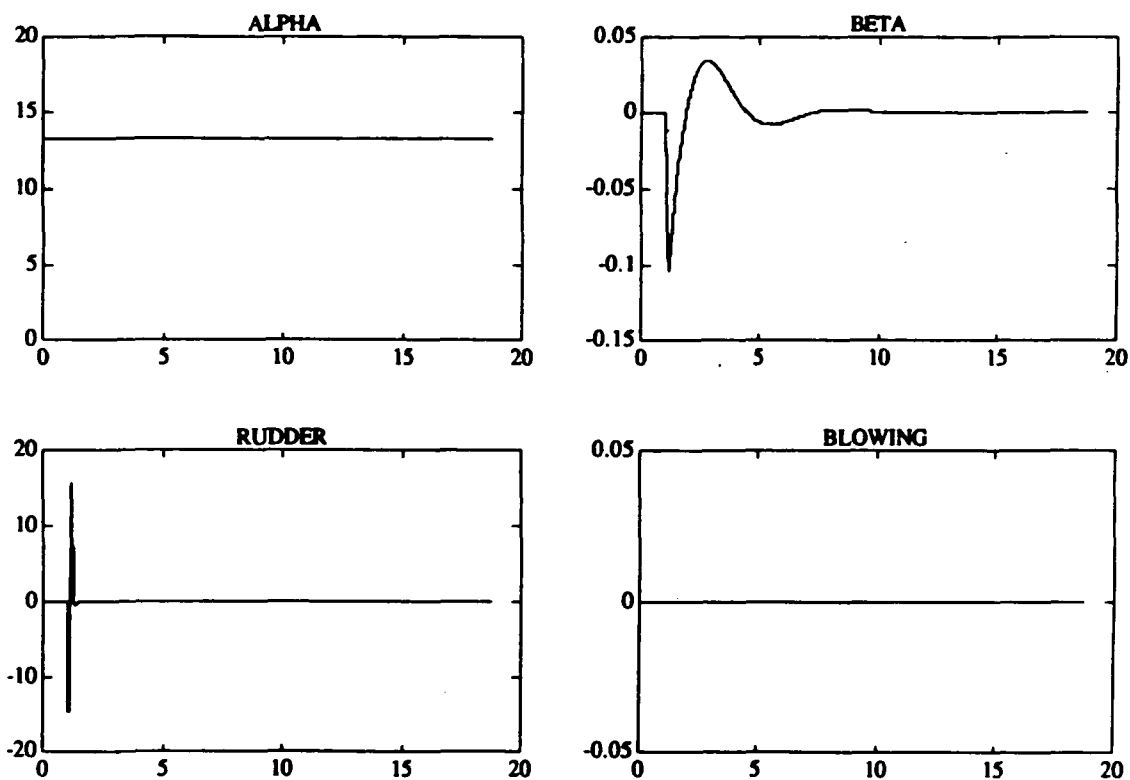


Figure 10. Time history of motion after rudder doublet input.  $\alpha = 13^\circ$

## PERFORMANCE OF HARV AT 45 deg

---

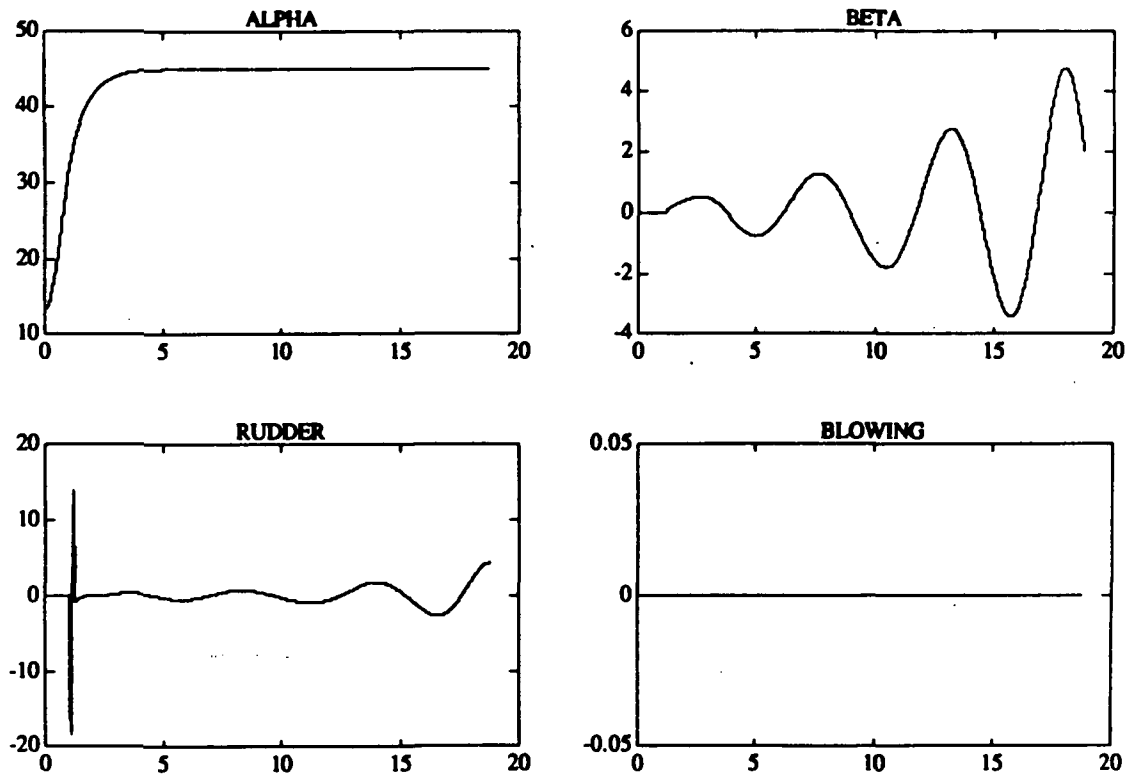


Figure 11. Time history of motion after rudder doublet input.  $\alpha = 45^\circ$

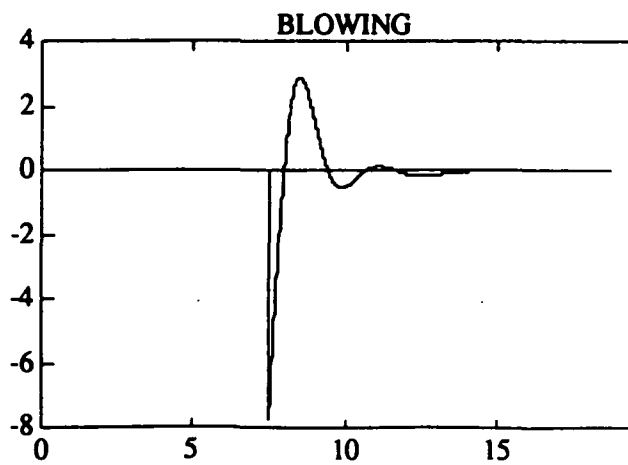
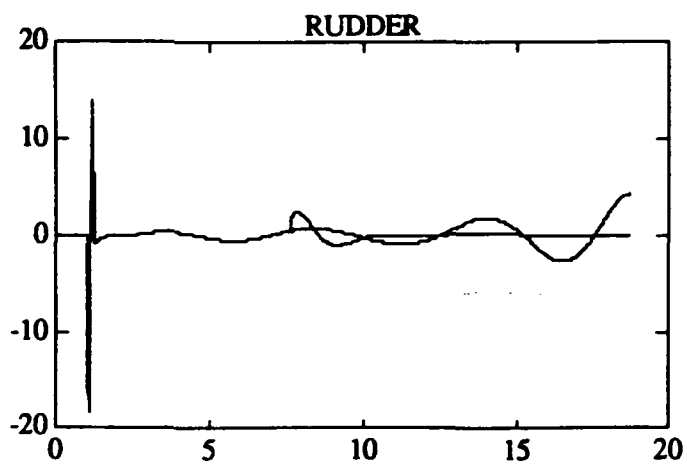
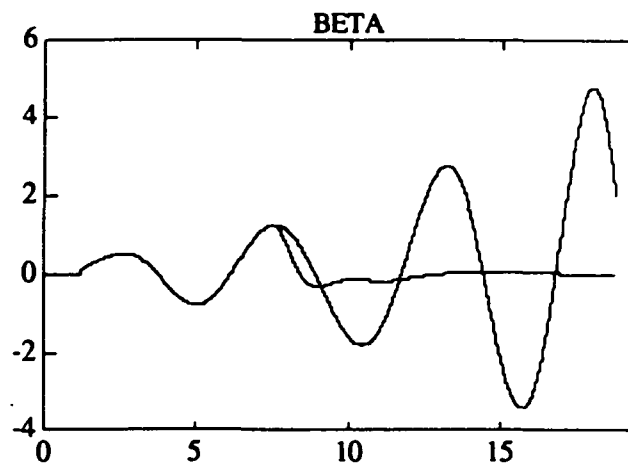
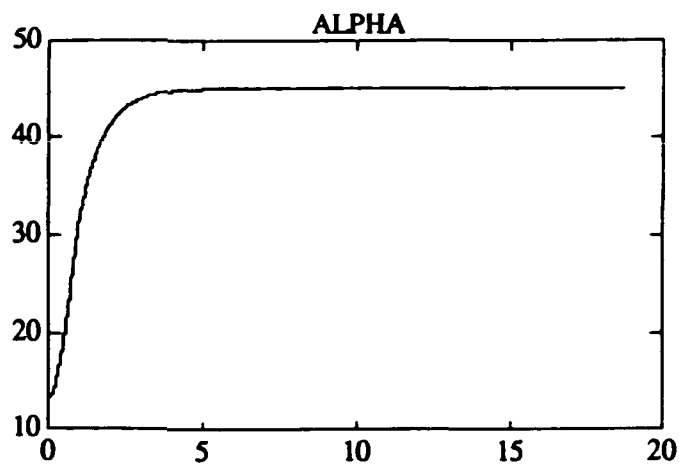


Figure 12. Time history of motion after rudder doublet input.  $\alpha = 45^\circ$   
Blowing control system on.

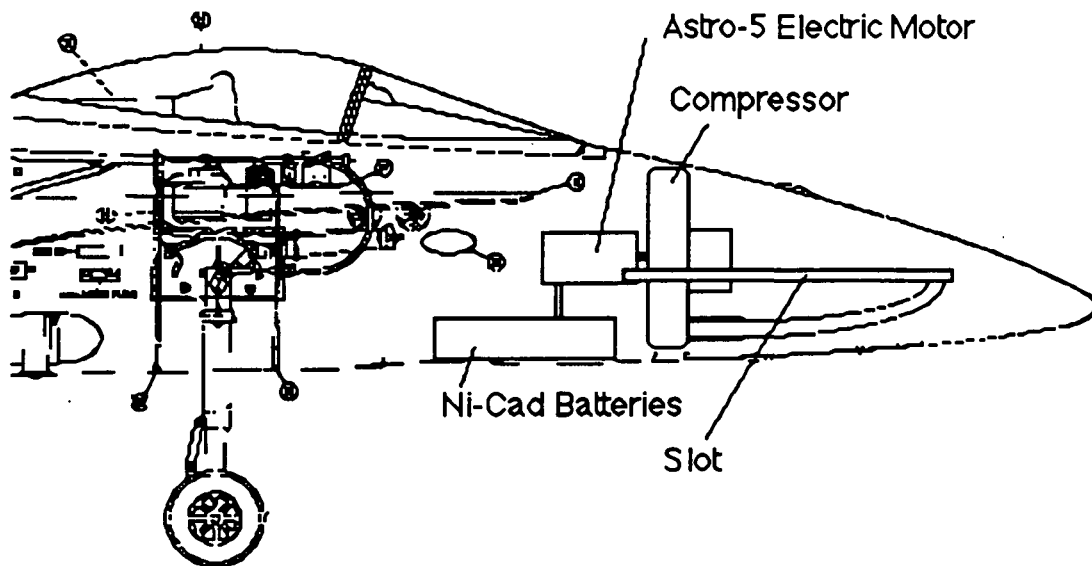
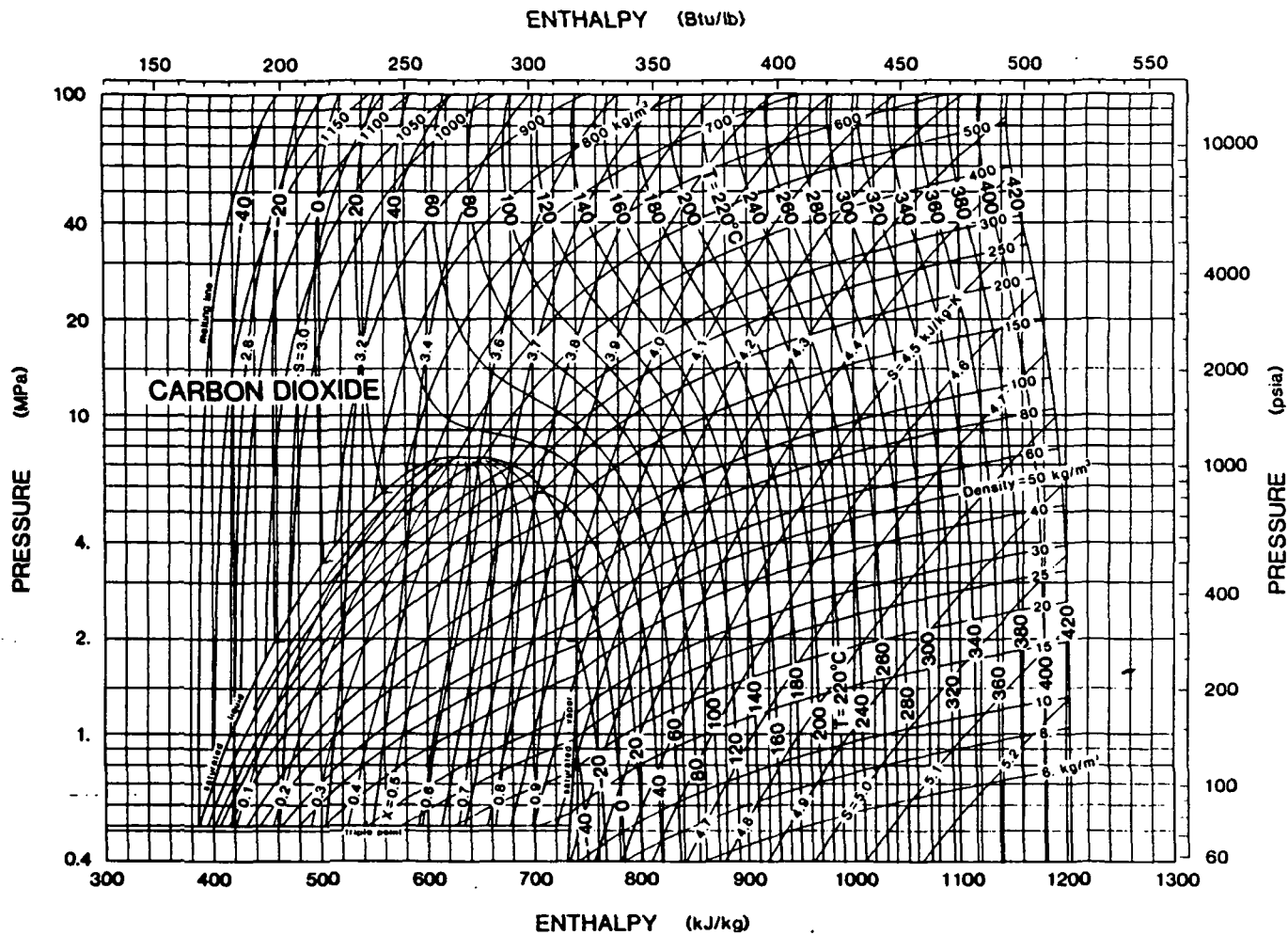


Figure 13. Installation of blowing system in F-18 model.





Figure 14. F-18 model installed in wind tunnel at Stanford University.



## EVALUATION OF BLOWING SYSTEM PARAMETERS

1989-10-09

12:49:55

CONTROL GAS - CO2

Cmu CL L/W Mj Tj [K] Vj [m/s] rhoj[kg/m3]

.005 1.0 1.0 .7 273. 181. 1.344

Aj [m2] l [m] h[mm] mdotj [kg/s] qS [N] Pa [Pa] ratio alt [ft]

.017 1.829 9.6 4.26 154252. 69693. 1.360 10000.

tblow [s] m0 [kg] vol [m3] rho0 [kg/m3] T0 [K] Qdot [kW]

600. 2553. 2.75 927. 273. 987.283

## EVALUATION OF BLOWING SYSTEM PARAMETERS

1989-10-09

12:49:02

CONTROL GAS - CO2

Cmu CL L/W Mj Tj [K] Vj [m/s] rhoj[kg/m3]

.005 1.8 1.0 .7 273. 181. 1.344

Aj [m2] l [m] h[mm] mdotj [kg/s] qS [N] Pa [Pa] ratio alt [ft]

.010 1.829 5.3 2.36 85696. 69693. 1.360 10000.

tblow [s] m0 [kg] vol [m3] rho0 [kg/m3] T0 [K] Qdot [kW]

600. 1418. 1.53 927. 273. 548.490

Tab.2

# VALUATION OF BLOWING SYSTEM PARAMETERS

989-08-16

3:08:47

CONTROL GAS - AIR

Cmu CL L/W Mj Tj [K] Vj [m/s] rhoj[kg/m3]

.005 1.0 1.0 .7 273. 232. .890

Aj [m2] l [m] h[mm] mdotj [kg/s] qS [N] Pa [Pa] ratio alt [ft]

.016 1.829 8.8 3.33 154252. 69693. 1.387 10000.

# VALUATION OF BLOWING SYSTEM PARAMETERS

989-08-16

3:09:53

CONTROL GAS - AIR

Cmu CL L/W Mj Tj [K] Vj [m/s] rhoj[kg/m3]

.005 1.8 1.0 .7 273. 232. .890

Aj [m2] l [m] h[mm] mdotj [kg/s] qS [N] Pa [Pa] ratio alt [ft]

.009 1.829 4.9 1.85 85696. 69693. 1.387 10000.

Tab.3

ORIGINAL PAGE IS  
OF POOR QUALITY

Table 4

PLA	W1	W25	P21 (total)	P3 (tot/static)	T25	T3
(°)	(lb/s)	(lb/s)	(psi)	(psi)	(°R)	(°R)
40	46	27	19	63/59	592	836
75	106	76	42	230/219	758	1203
87	127	96	52	311	819	1333

(PLA = Power Level Angle).

Table 5

PLA	W1	normal bleed	P3 (total/static)	T3
	(kg/s)	(kg/s)	( kPa )	(K)
40	20.9	1.25	434/407	464
75	48.1	2.88	1590/1510	668
87	57.6	3.46	2280/?	741

Table 6

PLA	W25	anti-ice bleed	$(p_3 - p_{21})/2$ + $p_{21}$	$(T_3 - T_{21})/2$ + $T_{21}$
	(kg/s)	(kg/s)	(kPa)	(K)
40	12.2	0.098	269	397
75	34.5	0.276	896	545
87	43.5	0.348	1250	598

```
PROGRAM RABLOW1
```

```
*
```

```
* RA AUG 1989
```

```
*
```

```
* Program for evaluating different parameters in fuselage blowing  
* scheme.
```

```
*
```

```
* Ken Craig 8/15/89
```

```
*
```

```
REAL Cmu,CL,LW,Mj,Tj,Vj,rhoj,Aj,l,h,mdotj,qS,Pa,ratio,  
#   tb,m0,vol,rho0,T0,R,gamma,alt,W,Qdot,delh  
INTEGER iload,igas  
INTEGER*2 IHR,IMIN,ISEC,I100TH,IYR,IMON,IDAY  
CHARACTER*64 outfile
```

```
*
```

```
WRITE(*,*) 'EVALUATION OF BLOWING SYSTEM PARAMETERS'  
WRITE(*,*) ' '
```

```
*
```

```
* OPEN OUTPUT FILE
```

```
*
```

```
WRITE(*,*) 'OUTPUT FILE :'  
READ(*, '(a)') outfile  
OPEN(1,FILE=outfile,STATUS='UNKNOWN',ACCESS='SEQUENTIAL',  
#IOSTAT=IOS,ERR=9000)  
WRITE(*,*) 'Blowing momentum coefficient Cmu :'  
READ(*,*) Cmu  
WRITE(*,*) 'Lift coefficient CL :'  
READ(*,*) CL  
WRITE(*,*) 'Load factor L/W :'  
READ(*,*) LW  
WRITE(*,*) 'Weight of aircraft'  
WRITE(*,*) '1      empty'  
WRITE(*,*) '2      fighter configuration'  
WRITE(*,*) '3      maximum'  
READ(*,*) iload  
GOTO (10,11,12), iload  
10 W = 9900*9.8  
GOTO 13  
11 W = 15740*9.8  
GOTO 13  
12 W = 23540*9.8  
13 qS = W*LW/CL  
WRITE(*,*) 'Altitude for manoeuver [ft] :'  
READ(*,*) alt
```

```
*
```

```
* CALL TABLE LOOKUP OF ISA FOR ATMOSPHERIC PRESSURE AT ALTITUDE
```

```
*
```

```
CALL TABISA(alt,Pa)  
WRITE(*,*) 'Jet Mach number Mj :'  
READ(*,*) Mj  
WRITE(*,*) 'Jet exit temperature Tj [K] :'  
READ(*,*) Tj  
WRITE(*,*) 'Jet slot lenght l [m] :'  
READ(*,*) l
```

```

WRITE(*,*) 'Choose control gas'
WRITE(*,*) '1   Air'
WRITE(*,*) '2   CO2'
READ(*,*) igas
GOTO (14,15),igas
*
* SECTION FOR AIR
*
14 gamma = 1.4
   R = 287.0
   Vj = SQRT(gamma*R*Tj)*Mj
   rhoj = Pa/R/Tj
   Aj = Cmu*qS/rhoj/Vj/Vj
   h = Aj/l
   mdotj = rhoj*Aj*Vj
   GOTO 100
*
* SECTION FOR CO2
*
15 gamma = 1.3
   R = 188.9
   Vj = SQRT(gamma*R*Tj)*Mj
*
* CALL TABLE LOOKUP FOR DENSITY of gas AT SPECIFIED TEMPERATURE
*
CALL TABCOG(Tj,rhoj)
Aj = Cmu*qS/rhoj/Vj/Vj
h = Aj/l
mdotj = rhoj*Aj*Vj
WRITE(*,*) 'Specify required blowing time, tb : '
READ(*,*) tb
m0 = mdotj*tb
WRITE(*,*) 'Specify reservoir storage temperature T0 [K] : '
READ(*,*) T0
*
* CALL TABLE LOOKUP FOR DENSITY of liquid and enthalpy of
vaporization
* AT SPECIFIED TEMPERATURE
*
CALL TABCOL(T0,rho0,delh)
vol = m0/rho0
Qdot = delh*mdotj
*
100 ratio = (1.0 + (gamma-1.0)/2.0*Mj*Mj)**(gamma/(gamma-1))
*
* WRITE RESULTS TO FILE AND SCREEN
*
CALL GETDAT(IYR,IMON,IDAY)
CALL GETTIM(IHR,IMIN,ISEC,I100TH)
WRITE(*,*) 'EVALUATION OF BLOWING SYSTEM PARAMETERS'
WRITE(*,*) ' '
WRITE(*,*) '(1X,I4.2,1H-,I2.2,1H-,I2.2)' IYR,IMON,IDAY
WRITE(*,*) '(1X,I2.2,1H:,I2.2,1H:,I2.2)' IHR,IMIN,ISEC
WRITE(*,*) ' '

```

```

      IF (igas.EQ.1) THEN
      WRITE(*,*) 'CONTROL GAS - AIR'
      ELSEIF (igas.EQ.2) THEN
      WRITE(*,*) 'CONTROL GAS - CO2'
      ENDIF
      WRITE(*,*) ' '
      WRITE(*,*) ' Cmu      CL      L/W      Mj      Tj [K]      Vj [m/s]
rhoj[kg/m3]'
      WRITE(*,*) ' '
      WRITE(*, '(1X,F5.3,2X,F3.1,3X,F3.1,2X,F3.1,4X,F4.0,4X,F4.0,
#          5X,F5.3)') Cmu,CL,LW,Mj,Tj,Vj,rhoj
      WRITE(*,*) ' '
      WRITE(*,*) ' Aj [m2] l [m] h[mm] mdotj [kg/s] qS [N] Pa [Pa]
rati
      #o alt [ft]'
      WRITE(*,*) ' '
      WRITE(*, '(1X,F5.3,4X,F5.3,1X,F4.1,2X,F5.2,8X,F7.0,1X,F6.0,
#          1X,F6.3,1X,F6.0)') Aj,l,h*1000.,mdotj,qS,Pa,ratio,alt
      WRITE(*,*) ' '
      IF (igas.EQ.2) THEN
      WRITE(*,*) ' tblow [s] m0 [kg] vol [m3] rho0 [kg/m3] T0 [K]
Qdot
      #[kW]'
      WRITE(*,*) ' '
      WRITE(*, '(2X,F4.0,6X,F5.0,3X,F5.2,4X,F5.0,9X,F4.0,3X,F8.3)')
#          tb,m0,vol,rho0,T0,Qdot
      ENDIF
      WRITE(1,*) 'EVALUATION OF BLOWING SYSTEM PARAMETERS'
      WRITE(1,*) ' '
      WRITE(1, '(1X,I4.2,1H-,I2.2,1H-,I2.2)') IYR,IMON,IDAY
      WRITE(1, '(1X,I2.2,1H:,I2.2,1H:,I2.2)') IHR,IMIN,ISEC
      WRITE(1,*) ' '
      IF (igas.EQ.1) THEN
      WRITE(1,*) 'CONTROL GAS - AIR'
      ELSEIF (igas.EQ.2) THEN
      WRITE(1,*) 'CONTROL GAS - CO2'
      ENDIF
      WRITE(1,*) ' '
      WRITE(1,*) ' Cmu      CL      L/W      Mj      Tj [K]      Vj [m/s]
rhoj[kg/m3]'
      WRITE(1,*) ' '
      WRITE(1, '(1X,F5.3,2X,F3.1,3X,F3.1,2X,F3.1,4X,F4.0,4X,F4.0,
#          5X,F5.3)') Cmu,CL,LW,Mj,Tj,Vj,rhoj
      WRITE(1,*) ' '
      WRITE(1,*) ' Aj [m2] l [m] h[mm] mdotj [kg/s] qS [N] Pa [Pa]
rati
      #o alt [ft]'
      WRITE(1,*) ' '
      WRITE(1, '(1X,F5.3,4X,F5.3,1X,F4.1,2X,F5.2,8X,F7.0,1X,F6.0,
#          1X,F6.3,1X,F6.0)') Aj,l,h*1000.,mdotj,qS,Pa,ratio,alt
      WRITE(1,*) ' '
      IF (igas.EQ.2) THEN
      WRITE(1,*) ' tblow [s] m0 [kg] vol [m3] rho0 [kg/m3] T0 [K]
Qdot

```



```

      #[kW]'
      WRITE(1,*) ' '
      WRITE(1,'(2X,F4.0,6X,F5.0,3X,F5.2,4X,F5.0,9X,F4.0,3X,F8.3)')
      #      tb,m0,vol,rho0,T0,Qdot
      ENDIF
      STOP
*
9000 WRITE(*,*) 'PROBLEM WITH OUTPUT FILE',IOS
      CLOSE(1)
      END

      SUBROUTINE TABCOG(T,rho)
      DIMENSION vol(8),Tg(8)
      DATA vol/10.64,11.14,11.63,12.12,12.61,13.10,13.60,14.09/
      DATA Tg/-20.0,0.0,20.0,40.0,60.0,80.0,100.0,120.0/
      N = 8
*
* CONVERT TEMPERATURE TO degF
*
      Tf = T*9.0/5.0 - 459.67
      CALL LOCATE(Tg,N,Tf,J)
*
* LINEAR INTERPOLATION
*
      volg = vol(J) + (vol(J+1)-vol(J))/(Tg(J+1)-Tg(J))*(Tf-Tg(J))
*
* CONVERT TO SI UNITS AND DENSITY
*
      rho = 1.601846E01/volg
      RETURN
      END

      SUBROUTINE TABCOL(T,rho,delh)
      DIMENSION dens(9),Tl(9),hl(9),hg(9)
      DATA dens/982.03,955.18,926.36,894.97,860.13,828.79,772.73
      #      724.83,604.70/
      DATA hl/479.01,490.47,502.38,514.84,528.04,539.33,558.14,
      #      572.84,604.89/
      DATA hg/738.07,736.4,733.96,730.58,725.98,721.1,710.73,
      #      700.33,668.3/
      DATA Tl/-10.0,-5.0,0.0,5.0,10.0,14.0,20.0,24.0,30.0/
      N = 9
*
* CONVERT TEMPERATURE TO degC
*
      Tc = T - 273.15
      CALL LOCATE(Tl,N,Tc,J)
*
* LINEAR INTERPOLATION
*
      #
      #      r h o = d e n s ( J )
      (dens(J+1)-dens(J))/(Tl(J+1)-Tl(J))*(Tc-Tl(J))
      hliq = hl(J) + (hl(J+1)-hl(J))/(Tl(J+1)-Tl(J))*(Tc-Tl(J))
      hgas = hg(J) + (hg(J+1)-hg(J))/(Tl(J+1)-Tl(J))*(Tc-Tl(J))

```

```
delh = hgas - hliq
RETURN
END
```

```
SUBROUTINE TABISA(alt,Pa)
DIMENSION pres(11),h(11)
DATA pres/10.132E4,8.987E4,7.948E4,7.01E4,6.163E4,5.4E4,
*      4.717E4,4.104E4,3.558E4,3.073E4,2.642E4/
DATA h/0.0,1E3,2E3,3E3,4E3,5E3,6E3,7E3,8E3,9E3,10E3/
N = 11
```

\*

\* CONVERT ALTITUDE TO m

\*

```
    altm = alt*3.048E-1
    CALL LOCATE(h,N,altm,J)
```

\*

\* LINEAR INTERPOLATION

\*

```
    Pa = pres(J) + (pres(J+1)-pres(J))/(h(J+1)-h(J))*(altm-h(J))
    RETURN
    END
```

```
SUBROUTINE LOCATE(XX,N,X,J)
```

```
DIMENSION XX(N)
```

```
JL=0
```

```
JU=N+1
```

```
10  IF(JU-JL.GT.1)THEN
```

```
    JM=(JU+JL)/2
```

```
    IF((XX(N).GT.XX(1)).EQV.(X.GT.XX(JM)))THEN
```

```
        JL=JM
```

```
    ELSE
```

```
        JU=JM
```

```
    ENDIF
```

```
GO TO 10
```

```
ENDIF
```

```
J=JL
```

```
RETURN
```

```
END
```